Optimising NMR Spectroscopy through Method and Software Development

Jonathan Yong

University of Oxford

Contents

refsection:1

refsection:2

refsection:3

refsection:4

Chapter 4

NOAH

chpt:noah

This final—and long—chapter describes my work on *NOAH* (NMR by Ordered Acquisition using ^{1}H detection) *supersequences*, pulse sequences which record multiple 2D datasets (‘*modules*’) in the time required for one. This is an attractive NMR technique for several reasons: the time savings are clearly a key factor, but the flexibility of being able to combine almost any set of modules also makes NOAH supersequences applicable to a variety of contexts.

I begin by introducing the concepts underlying NOAH supersequences, as well as a general discussion of the time savings (and sensitivity per unit time) benefits thus realised. I then describe the GENESIS (GENEration of Supersequences In Silico) website, which allows users to generate Bruker pulse programmes for almost every imaginable NOAH supersequence. After this, my work on various aspects of the actual sequences themselves is described, with a special focus on newly developed and/or improved modules. Finally, the design of ‘parallel’ supersequences which use interleaved and/or time-shared modules is discussed.

This work was done in close collaboration with Ēriks Kupče (Bruker UK). However, all results and analysis shown in this chapter are mine, unless explicitly stated. The work in this chapter forms the subject of several publications:

- Yong, J. R. J.; Hansen, A. L.; Kupče, Ē.; Claridge, T. D. W. Increasing sensitivity and versatility in NMR supersequences with new HSQC-based modules. *J. Magn. Reson.* **2021**, *329*, 107027, DOI: 10.1016/j.jmr.2021.107027
- Kupče, Ē.; Yong, J. R. J.; Widmalm, G.; Claridge, T. D. W. Parallel NMR Supersequences: Ten Spectra in a Single Measurement. *JACS Au* **2021**, *1*, 1892–1897, DOI: 10.1021/jacsau.1c00423
- Yong, J. R. J.; Kupče, Ē.; Claridge, T. D. W. Modular Pulse Program Generation for NMR Supersequences. *Anal. Chem.* **2022**, *94*, 2271–2278, DOI: 10.1021/acs.analchem.1c04

964

- Yong, J. R. J.; Kupče, Ē.; Claridge, T. D. W. Uniting Low- and High-Sensitivity Experiments through Generalised NMR Supersequences. **2022**, manuscript in preparation

The material in the introductory sections also closely follow two reviews which I have contributed to:

- Kupče, Ē.; Frydman, L.; Webb, A. G.; Yong, J. R. J.; Claridge, T. D. W. Parallel nuclear magnetic resonance spectroscopy. *Nat. Rev. Methods Primers* **2021**, *1*, No. 27, DOI: 10.1038/s43586-021-00024-3
- Yong, J. R. J.; Kupče, Ē.; Claridge, T. D. W. In *Fast 2D solution-state NMR: concepts and applications*, Giraudeau, P., Dumez, J.-N., Eds., forthcoming, 2022

4.1 Introduction

sec:noah__introduction

The characterisation of small molecules and biomolecules by NMR spectroscopy relies on a suite of standard 2D NMR experiments, which seek to detect heteronuclear scalar couplings (e.g. HSQC and HMBC), homonuclear scalar couplings (e.g. COSY and TOCSY), or through-space interactions (e.g. NOESY and ROESY). Although 2D experiments provide far superior resolution and information content compared to 1D spectra, they also require substantially longer experiment durations, as the indirect dimension must be constructed through the acquisition of many t_1 increments. This problem is further exacerbated by the fact that structural elucidation or verification often necessitates the acquisition of several different 2D experiments.

The acceleration of 2D NMR has thus proven to be a popular area of research. We may broadly categorise existing techniques into two classes: firstly, those which seek to directly speed up the acquisition of *individual* 2D spectra, and secondly, *multiple-FID* experiments which aim to collect two or more 2D spectra in the time required for one.* The former category includes methods such as non-uniform sampling (NUS),[7–10] fast pulsing (i.e. shortening of recovery delays),[11–14] ultrafast NMR,[5,15–19] Hadamard encoding,[20,21] and spectral aliasing;[22–24] whereas the latter encompasses time-shared NMR,[25,26] multiple-receiver NMR,[27–29] and—of course—NOAH supersequences.[5,30,31]

The scope of this introductory section will be limited to only NOAH supersequences. However, many of these techniques are closely related, and I will introduce concepts from elsewhere as needed. It should be noted that there are several other multiple-FID experiments which, while not explicitly advertised as such, are conceptually identical to NOAH experiments.[32–35] I do not discuss these here.

4.1.1 Time savings and sensitivity analyses

subsec:noah__snr

In a typical 2D NMR experiment, the majority of the experiment duration is taken up by the *recovery delay*—the time required for spins to return to their equilibrium polarisation, such that the next transient or t_1 increment can be recorded. The removal (or shortening) of recovery delays is thus a very effective way of speeding up 2D data acquisition. In NOAH supersequences, 2D experiments ('modules') can be directly concatenated without the addition of extra recovery delays between them (FIG): only one overall recovery delay is required for the entire supersequence. This means that, to a first approximation, a supersequence containing N modules ($N \geq 2$) can be acquired in the time needed for just one module.

*These are by no means mutually exclusive: many of the techniques here can be combined to provide even greater efficiency.

To be more precise, we can express the experiment duration, τ_{exp}, as a sum of its parts:

$$\tau_{\text{exp}} = \tau_{\text{ps}} + \tau_{\text{acq}} + d_1, \tag{4.1}$$ {eq:exp_duration_2d}

where τ_{ps} is the time required for the pulse sequence itself (typically several milliseconds), τ_{acq} is the acquisition time (several hundred milliseconds), and d_1 is the recovery delay (one or more seconds). The *time-saving factor* ρ_t for a NOAH supersequence, as compared to a series of conventional standalone experiments, is then:

$$\rho_t = \frac{\sum_i \tau_{\text{conv}}^{(i)}}{\tau_{\text{NOAH}}} = \frac{\sum_i (\tau_{\text{ps}}^{(i)} + \tau_{\text{acq}}^{(i)} + d_1^{(i)})}{d_1 + \sum_i (\tau_{\text{ps}}^{(i)} + \tau_{\text{acq}}^{(i)})}, \tag{4.2}$$ {eq:rho_t}

where τ_{NOAH} is the duration of the NOAH experiment, τ_{conv} is the duration of a conventional experiment, and the superscript (i) represents the i-th module or conventional experiment being acquired. The sum runs from $i = 1$ to N, where N is the number of modules. If we assume that $d_1^{(i)} = d_1$ is the same for all N conventional experiments and the supersequence, then in the limit where

$$d_1 \gg \sum_i \tau_{\text{ps}}^{(i)} + \tau_{\text{acq}}^{(i)}, \tag{4.3}$$ {eq:d1_limit}

we have that $\rho_t \to N d_1 / d_1 = N$. This analysis makes plenty of assumptions, and is not entirely valid in practice. For example, *each* τ_{acq} is often around 5–10% of d_1, so is not entirely negligible, especially in longer supersequences. Furthermore, some modules require longer τ_{ps}: most notable is the NOESY module, which contains a mixing time of several hundred milliseconds. (HMBC, TOCSY, and ROESY spectra are also lesser offenders.) These factors serve to reduce ρ_t from its idealised value of N; generally, this deviation is larger as N increases, because eq. (4.3) becomes less and less valid. Nevertheless, the general point that time savings are approximately proportional to N stands.

For relatively concentrated samples, where sensitivity is not an issue, we can in fact end the discussion here. In this *sampling-limited regime*, the minimum 2D experiment duration is dictated purely by the number of t_1 increments needed to obtain sufficient resolution in the indirect dimension, as well as the minimum phase cycle required for artefact suppression.* NOAH supersequences are identical to conventional experiments in both aspects, but provide a time-saving factor of $\rho_t \sim N$.

The development of modern NMR instrumentation, including high-field magnets and cryogenic probes, means that the sampling-limited regime continues to be extended to ever lower concentrations. However, it is often not this simple: the opposite *sensitivity-limited regime* is still very

*With modern gradient-enhanced experiments, the minimum phase cycle may well not even be a 'cycle'; see also fig. 1.8.

commonly encountered, for example with naturally insensitive experiments (e.g. ADEQUATE), low-field benchtop NMR, or most simply, dilute samples.*

In such cases, it becomes mandatory to compare the SNRs of the NOAH modules and conventional experiments. To do so, we define for each module an *SNR factor* $A^{(i)}$, which is the SNR of the NOAH module divided by the SNR of a conventional experiment, acquired with the same parameters.* In general, we have that $A \leq 1$, because NOAH modules frequently contain small modifications from conventional experiments (as will be explained in § 4.1.2). The *gain in sensitivity per unit time*, $\varepsilon^{(i)}$, is then defined by

$$\varepsilon^{(i)} = A^{(i)}\sqrt{\rho_t}, \tag{4.4}$$ {eq:varepsilon_i}

where the square root accounts for the fact that SNR scales only as the square root of the number of scans, or the number of times the experiment can be repeated in a given period. Of course, the exact values calculated for $A^{(i)}$ (and hence $\varepsilon^{(i)}$) will depend on the sample chosen for the comparison. These values should therefore be assumed to be valid only for similar samples.

If $\varepsilon^{(i)} > 1$, as is frequently the case, this means that the NOAH supersequence provides greater sensitivity per unit time in the i-th module compared to a standalone experiment. Equivalently, performing a NOAH experiment allows data of sufficient sensitivity to be obtained in less time. Naturally, this condition is most important for modules which are inherently insensitive, particularly heteronuclear correlation modules. For sensitive (typically homonuclear) modules, it is often perfectly tolerable to have $A < 1$ or even $\varepsilon < 1$, as even with this sensitivity penalty they are still more intense than the heteronuclear modules.

Another issue with NOAH supersequences is that each module is run with the same number of scans (phase cycle). Although this was touted as a benefit in the sampling-limited regime, this may in fact be undesirable in the sensitivity-limited regime, where insensitive experiments need to be run with more scans than sensitive ones. In this case, the *effective* time savings provided by NOAH experiments are smaller:

$$\rho_{t,\mathrm{eff}} = \frac{\sum_i \tau_{\mathrm{conv}}^{(i)}}{\tau_{\mathrm{NOAH}}} = \frac{\sum_i S^{(i)}(\tau_{\mathrm{ps}}^{(i)} + \tau_{\mathrm{acq}}^{(i)} + d_1^{(i)})}{Sd_1 + S\sum_i(\tau_{\mathrm{ps}}^{(i)} + \tau_{\mathrm{acq}}^{(i)})}, \tag{4.5}$$ {eq:rho_t_eff}

where each standalone experiment is acquired with $S^{(i)}$ scans and the NOAH experiment with S scans. Typically, S is simply the largest of the $S^{(i)}$. If $S^{(i)} = S$ for all i, then eq. (4.5) simply reduces

*If the SNR factor $A^{(i)}$ as discussed below is *very small*, then it is possible that even concentrated samples may be shifted into the sensitivity-limited regime. This is never really the case in practice, though, as will be shown in § 4.1.3.

*The relative SNR will likely vary from peak to peak in the spectrum, and $A^{(i)}$ should in theory be quoted either as an average over all peaks, or as a range. This is what I have done in this thesis. However, comparisons in the literature are not always as thorough.

to eq. (4.2); on the other hand, if the $S^{(i)}$'s are different, then we have that $\rho_{t,\text{eff}} < \rho_t$. In such a situation, it is probably more appropriate to describe a NOAH supersequence as 'measuring the most insensitive module and getting the others for free'. Indeed, if $S = S^{(i)} \gg S^{(j\neq i)}$, then 'the other' modules require almost no time to measure (relative to the least sensitive module), and $\rho_{t,\text{eff}}$ tends towards 1, meaning that even the time-saving utility of NOAH vanishes. A corollary of this is that NOAH supersequences are generally best constructed from modules which have similar intrinsic sensitivities and hence similar $S^{(i)}$'s.

As the reader can no doubt appreciate by now, the comparison of NOAH and conventional spectra is fraught with subtleties (which are sometimes glossed over in the literature, but invariably surface in real-life discussions). In fact, it is hardly even difficult to construct yet more edge cases. For example, one may not want to acquire all the individual spectra 'conventionally': for example, NUS may be used for a HSQC experiment but not for others; or d_1 may be varied for different experiments. These will have an impact on both the durations of the experiments, as well as their sensitivities. To make any meaningful quantitative comparisons, it is therefore necessary to restrict the discussion to values of ρ_t, A, and ε, which can be objectively calculated. This is the approach I have taken in this thesis. These should of course be read with the qualitative understanding that depending on the context, these aforementioned factors may lead to *some*—but never a *complete*—decrease in the utility of NOAH experiments.

4.1.2 Magnetisation pools

subsec:noah__magpools

Having gotten this relatively dry material out of the way, I now turn to exactly how NOAH supersequences are constructed. Ordinarily, if the recovery delay is removed from an NMR experiment, its sensitivity will be greatly reduced because insufficient magnetisation will have recovered between repetitions; or in other words, $A^{(i)}$ will be very small. Such experiments would only really be useful well in the sampling-limited regime.

The key to avoiding this in NOAH supersequences is to make sure that *each module samples a different source of magnetisation*. For example, a HSQC module can be designed to only sample magnetisation of protons directly bonded to the 1.1%-natural abundance ^{13}C, and leave all other proton magnetisation untouched. Immediately following this, the remainder of the proton magnetisation can then be used to record (say) a COSY module, without needing a separate recovery delay. Using the notation of Orts and Gossert,[36] the magnetisation of ^{13}C–bound protons is denoted as $^1\text{H}^\text{C}$, and the magnetisation of protons *not* bonded to ^{13}C is denoted as $^1\text{H}^{!\text{C}}$. Protons not directly bonded to NMR-active heteronuclei are labelled $^1\text{H}^{!\text{X}}$, and will often be referred to as 'bulk' magnetisation, since (in natural-abundance samples) the majority of protons fall into this category.

Most standard 2D experiments do not preserve unused magnetisation but instead dephase it through CTP gradient selection; thus, NOAH modules often require some modifications compared to standard experiments. For example, compared to the echo–antiecho HSQC (discussed in § 1.4.5), the NOAH HSQC module[30] adds an extra CTP gradient so that the bulk magnetisation is refocused and ultimately returned to the $+z$ equilibrium state (fig. 4.1). (This is largely identical to the 'symmetrised' ASAP-HSQC experiment.[37])

fig:noah_hsqc

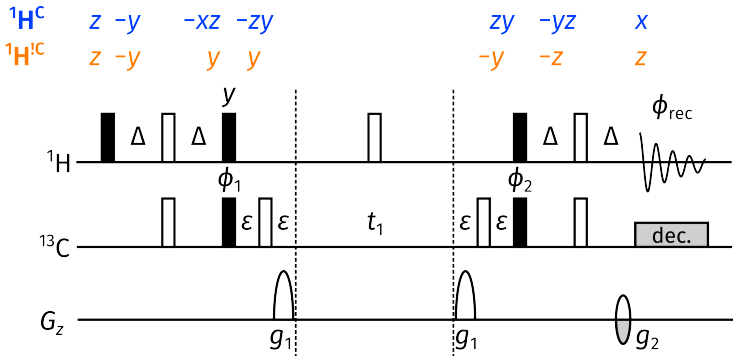

Figure 4.1: NOAH HSQC module. The delay Δ is set to $1/(4 \cdot {}^1J_{\mathrm{CH}})$. Phase cycling is performed with $\phi_1 = (x, -x)$, $\phi_2 = (x, x, -x, -x)$, and $\phi_{\mathrm{rec}} = (x, -x, -x, x)$. Gradient amplitudes are $(g_1, g_2) = (80\%, \pm 40.2\%)$. The notation for product operator analysis is explained in the *Preface*.

Sometimes, the modifications required are more extensive, as in the HMBC module. If this module is followed by a HSQC module (or any other module which draws on ${}^1\mathrm{H}^{\mathrm{C}}$ magnetisation), the initial 90° excitation pulse must be replaced with a *zz*-filter (fig. 4.2). This performs an *isotope-selective rotation* in that ${}^1\mathrm{H}^{\mathrm{C}}$ magnetisation is stored along the *z*-axis, but ${}^1\mathrm{H}^{\mathrm{!C}}$ magnetisation is excited (and subsequently detected). In general, sequences which are thus modified have lower sensitivities (i.e. $A < 1$) than the 'original' sequences from which they were derived.

fig:noah_hmbc_no90_po

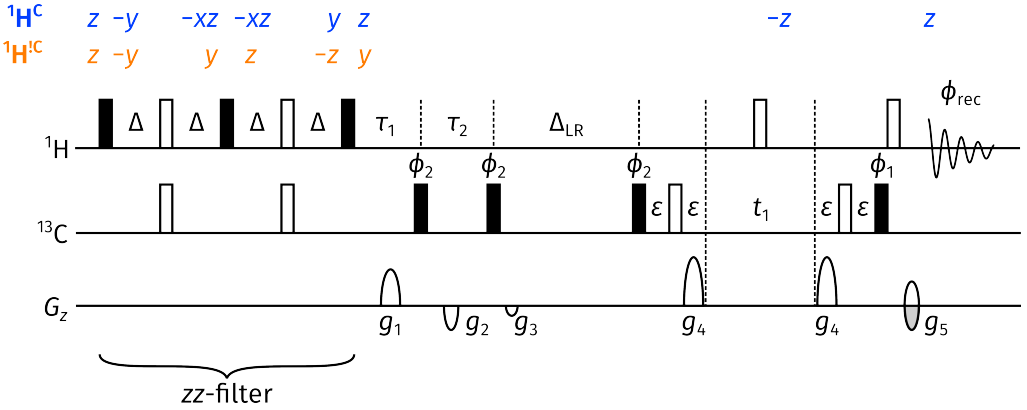

Figure 4.2: NOAH HMBC module. Delays are set as: $\Delta = 1/(2 \cdot {}^nJ_{\mathrm{CH}})$; $\tau_1 = 1/(2 \cdot {}^1J_{\mathrm{CH,max}})$; $\tau_2 = 1/(2 \cdot {}^1J_{\mathrm{CH,min}})$ (see also § 3.4.7). Phase cycling is performed with $\phi_1 = (x, -x)$, $\phi_2 = (x, x, -x, -x)$, and $\phi_{\mathrm{rec}} = (x, -x, -x, x)$. Gradient amplitudes are $(g_1, g_2, g_3, g_4, g_5) = (15\%, -10\%, -5\%, 80\%, \pm 40.2\%)$.

In contrast, modules placed towards the *end* of a supersequence do not need to be modified, as they do not need to preserve any magnetisation. This includes virtually all homonuclear modules, which are allowed to simply consume any remaining magnetisation. Although this makes their implementation very straightforward, in general these modules will *also* suffer some losses in sensitivity, because the preceding modules do not perfectly retain all magnetisation.

Thus, in general, it is not possible for any module in a NOAH supersequence to have $A = 1$, unless it is placed first in the supersequence *and* has not undergone any modifications.* Such cases are very rare, and it is thus necessary to accept some decreases in A, which are often fairly small (on the order of 10–20%). In the sampling-limited regime, sensitivity is not at a premium and this is often perfectly tolerable. In the sensitivity-limited regime, the full time savings ρ_t cannot be realised, but since ε is still typically larger than 1, there is still an overall boost in sensitivity per unit time.

4.1.3 Case studies

sec:noah__case_studies

Using all that has been described in the previous sections, we now look at a few 'typical' supersequences to understand their construction. A quick note about the nomenclature of NOAH supersequences is warranted here. Supersequences are labelled by the number of modules N, plus a series of single-letter codes corresponding to the identity and ordering of the modules involved (table 4.1). Occasionally, superscripts or subscripts are used to qualify the modules involved.† Thus, a NOAH supersequence containing three modules—say ^{15}N HMQC, ^{13}C HSQC, and CLIP-COSY—would be referred to as a NOAH-3 $\mathrm{M_N SC^c}$. Table 4.2 provides values of ρ_t and A for each module of several typical supersequences, which will be rationalised in the text which follows.

NOAH-2 SC: HSQC + COSY

We begin with perhaps the simplest example of a NOAH supersequence, one containing the HSQC and COSY modules: this is labelled as a NOAH-2 SC experiment (entry 1, table 4.2). As shown in fig. 4.1, the HSQC module only samples $^1\mathrm{H}^{\mathrm{C}}$ magnetisation, and leaves $^1\mathrm{H}^{!\mathrm{C}}$ magnetisation along the $+z$-axis Although the HSQC experiment has to be modified to preserve this $^1\mathrm{H}^{!\mathrm{C}}$ magnetisation, its sensitivity is practically unaffected as compared to a 'standard' HSQC

*Of course, this also depends on exactly *what* standalone experiment the NOAH supersequence is being compared against. Sometimes, in the literature, the NOAH experiment has been compared against its constituent modules acquired in a standalone fashion; in this case, the first module will always have $A = 1$. This tells us how much we gain through the act of concatenating modules, but is less meaningful in the 'real world' where one is interested in how useful NOAH is relative to 'typical' optimised 2D experiments. I therefore prefer to make comparisons against standard-library sequences.

†With the increasing number of modules, and the variety of modern NMR experiments which could be incorporated into NOAH supersequences, keeping these abbreviations short yet meaningful has been a challenge.

^{1}H–^{15}N modules		^{1}H–^{13}C modules		^{1}H–^{1}H modules	
Module	Code	Module	Code	Module	Code
HMQC	M_N	HSQC	S	COSY	C
HSQC	S_N	seHSQC	S^+	CLIP-COSY	C^c
seHSQC	S_N^+	HSQC-TOCSY	S^T	DQF-COSY	C
HMBC	B_N	HSQC-COSY	S^C	TOCSY	T
		2BOB	O	NOESY	N
		HMBC	B	ROESY	R
		ADEQUATE	A	PSYCHE	P
				TSE-PSYCHE	P^T
				PSYCHE 2DJ	J

tbl:noah_modules

Table 4.1: A (non-exhaustive) list of single-letter module codes for a selection of NOAH modules. Note that, in the literature, the ^{15}N HMQC module has been referred to simply by 'M', since the HSQC module is preferred for ^{1}H–^{13}C correlations. In this thesis, I include the subscript N throughout to avoid any ambiguity.

Entry	Sequence	τ_{NOAH}	ρ_t	A				
				HMBC	seHSQC	HSQC	COSY	TOCSY
1	SC	15 min 0 s	1.87			0.97	0.90	
2	SCT	16 min 25 s	2.60			1.01	0.99	0.79
3	BS	15 min 40 s	1.82	0.93		0.87		
4	SB	15 min 35 s	1.83	0.99		0.96		
5	BSCT	17 min 48 s	3.22	0.95		0.90	0.36	0.28
6	BS_N^+SCT	18 min 57 s	3.74	0.95	0.71	0.66	0.38	0.30
7	S_N^+BSCT	18 min 56 s	3.75	0.76	0.79	0.74	0.33	0.26

tbl:noah_sensitivities

Table 4.2: Sensitivity and time-saving analyses of several typical NOAH supersequences. All experiments were acquired with 2 scans per increment, 256 t_1 increments, an acquisition time of 67 ms, and a recovery delay of 1.5 s. The following Bruker library sequences were used as the 'conventional' experiments: `hmbcetgpl2nd`, `hsqcetf3gpsi2`, `hsqcetgpsp.2`, `cosygpqf`, and `dipsi2gpphzs`. *Data code:* `7Z-220224`.

($A = 0.97$). Furthermore, the COSY module retains *most* of its sensitivity ($A = 0.90$). The small loss here is because the HSQC module does not *perfectly* preserve the $^1H^{!C}$ magnetisation: for example, evolution of J-couplings as well as relaxation occur during the HSQC pulse sequence, which are ignored in the product operator analysis in fig. 4.1.

The value of the time-saving factor, $\rho_t = 1.87$, is very close to the theoretical limit of $N = 2$. This reflects the fact that the pulse sequence itself, τ_{ps}, is fairly short for both the HSQC and COSY modules; the deviation therefore chiefly arises from the acquisition time, τ_{acq}. In all respects, this is therefore an example of an 'ideal' NOAH supersequence, where the combination of two modules provides time savings without compromising on sensitivity.

It is worth pointing out that the order of the modules cannot be reversed: the COSY module cannot be (easily) modified to preserve $^{1}H^{C}$ magnetisation. In a hypothetical NOAH-2 CS supersequence, the later HSQC module would only be able to use magnetisation recovered during the COSY FID, leading to substantial sensitivity drops.

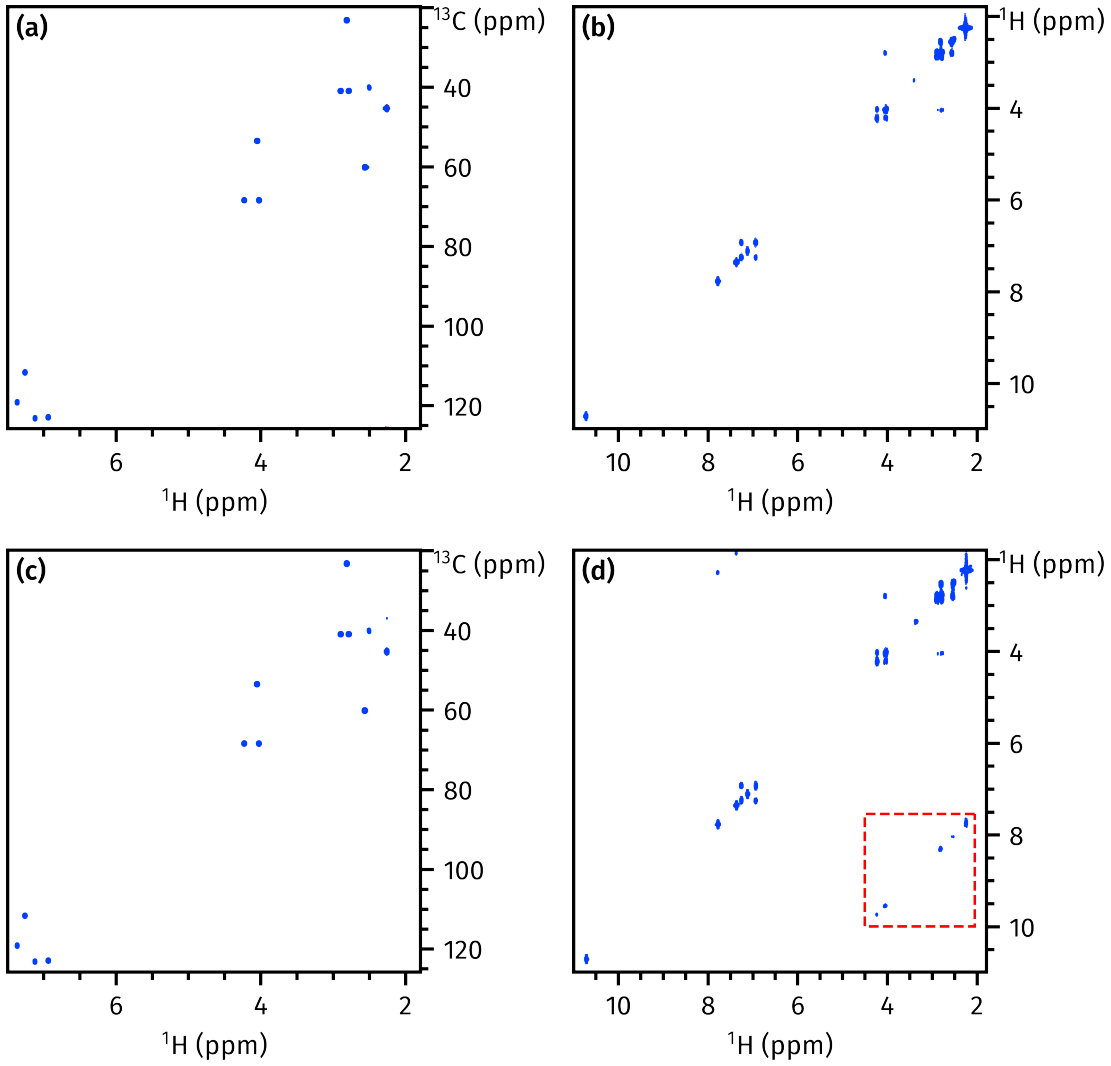

Figure 4.3: **(a)** HSQC from NOAH-2 SC supersequence. **(b)** COSY from NOAH-2 SC supersequence. **(c)** Standalone HSQC. **(d)** Standalone COSY; off-diagonal artefacts are highlighted in the red box. *Data code:* `7Z-220224`.

A final point to consider would be whether the NOAH data has comparable spectral quality in terms of (for example) artefacts. In this case, the answer is yes: the NOAH HSQC spectrum is virtually identical to the standalone (figs. 4.3a and 4.3c; both spectra have low-level artefacts of different kinds, which do not seriously impede the interpretation and are not shown). On the other hand, the NOAH COSY spectrum seems to actually *improve* on the standalone COSY, in that it better suppresses off-diagonal artefacts (figs. 4.3b and 4.3d). These artefacts likely arise in the standalone COSY because of accidental refocusing of magnetisation which has not completely

relaxed between t_1 increments.[38] In contrast, the NOAH COSY module has an extra set of HSQC gradients between every repetition of the COSY, so accidental refocusing is less likely. (Similar artefacts have been noted before in the DQF-COSY experiment,[39,40] and have also shown to be attenuated in the corresponding NOAH module.[41]) That said, such improvements are not always guaranteed: there are sometimes artefacts which arise uniquely in NOAH experiments, some of which are discussed in the following sections.

NOAH-3 SCT: HSQC + COSY + TOCSY

Evidently, the fact that the HSQC preserves almost all $^1H^{!C}$ magnetisation means that *any* homonuclear module—or a combination thereof—can be placed after it. In general, since homonuclear modules tend to consume any remaining bulk magnetisation, it is very difficult to create combinations of homonuclear modules which do not lead to significant reductions in sensitivity. The only real exceptions are COSY/X combinations, where X can be NOESY, ROESY, or TOCSY: instead of concatenating the COSY and X modules, the COSY pulse sequence can instead be nested *within* the X module, as was first demonstrated with X = NOESY.[42,43] Here, we use the COSY/TOCSY combination as an example.[44] The COSY, TOCSY, and combined COSY/TOCSY modules are shown in fig. 4.4.

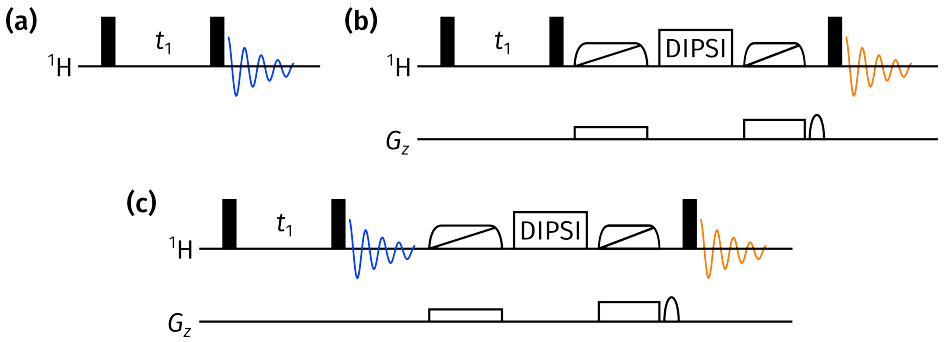

Figure 4.4: **(a)** COSY module. **(b)** TOCSY module; zero-quantum suppression is employed before and after the isotropic mixing period. **(c)** Combined COSY/TOCSY module, where the COSY FID is acquired immediately before the TOCSY mixing.

As shown in table 4.2 (entry 2), this nesting of the COSY module does not materially affect the TOCSY sensitivity. A small loss of approximately 20% is observed, which is partly due to the imperfect magnetisation preservation by the HSQC, and perhaps also due to relaxation during the COSY acquisition period. As for the time-saving factor, a slightly larger deviation ($\rho_t = 2.60$) is observed from the ideal value of 3. This reflects the addition of a TOCSY mixing period, which contributes to τ_{ps}.

NOAH-2 BS: HMBC + HSQC

As mentioned previously, the HMBC module shown in fig. 4.2 is designed to retain $^{1}H^{C}$ magnetisation through the addition of the *zz*-filter. This can be used in a subsequent HSQC module in a NOAH-2 BS supersequence. Entry 3 of table 4.2 shows that the addition of the *zz*-filter to eh HMBC causes a relatively small 7% decrease in sensitivity; on the other hand, the HSQC loses 13% of its sensitivity because of incomplete magnetisation preservation.

Generally, it has been recommended that less sensitive modules are placed earlier in the supersequence so that they can access a larger proportion of the equilibrium magnetisation. Since the HMBC is less sensitive of the two modules, this rule of thumb suggests that the BS supersequence would be better than the alternative SB supersequence. In fact, the opposite is true, as entry 4 of table 4.2 shows. The HSQC module has a boost in sensitivity because it is placed first in the supersequence, and no longer needs to rely on the $^{1}H^{C}$ magnetisation preserved by the HMBC; and the HMBC also benefits because the *zz*-filter modification is no longer needed. Arguably, the ordering of modules in a supersequence should be considered on a case-by-case basis.

NOAH-4 BSCT: HMBC + HSQC + COSY + TOCSY

We now move on to a longer supersequence containing four modules, with a correspondingly larger ρ_t value of 3.22. The sensitivity of the HSQC module is practically the same as in the NOAH-2 BS supersequence just described: however, the COSY and TOCSY modules expose one weakness of the HMBC module which has so far been overlooked. In principle, the HMBC module should only excite magnetisation of protons which are long-range coupled to ^{13}C (which we could, for example, denote as $^{1}H^{C(LR)}$). This magnetisation pool should be separate from both the directly coupled protons ($^{1}H^{C}$), as well as protons which are not coupled to any ^{13}C at all ($^{1}H^{!C}$). Unfortunately, this is not the case: it is not actually possible to separate the $^{1}H^{C(LR)}$ and $^{1}H^{!C}$ magnetisation pools. The HMBC excites both of these magnetisation sources, dephases the latter using CTP gradients, and detects the signal arising from the former.

What this means, of course, is that the COSY/TOCSY module which rely on $^{1}H^{!C}$ magnetisation will have substantially lower sensitivities. The signal detected in these two modules derives only from whatever has recovered during the previous two acquisition periods, as shown in entry 5 of table 4.2: A for COSY and TOCSY is 0.36 and 0.28 respectively. That said, this is in fact not likely to be an issue *even* for sensitivity-limited samples. Because the intrinsic sensitivity of the HMBC is orders of magnitude lower than the COSY and TOCSY, even with these large losses in sensitivity, the COSY and TOCSY spectra still have greater intensities than the HMBC. Thus, as long as the entire supersequence is acquired with enough scans to make the HMBC SNR sufficient, the SNR in the COSY and TOCSY will *also* be acceptable. This is illustrated in fig. 4.5.

A rather more insidious problem is that different signals relax at different rates: thus, the COSY and TOCSY spectra (or indeed, any homonuclear module) will have uneven intensities and are frequently asymmetric. This can be seen in the COSY spectrum, where a pair of asymmetric crosspeaks are highlighted. Adding a period of isotropic mixing before the COSY module[45] can help to ameliorate this to some extent (this was not performed when acquiring the data in fig. 4.5).

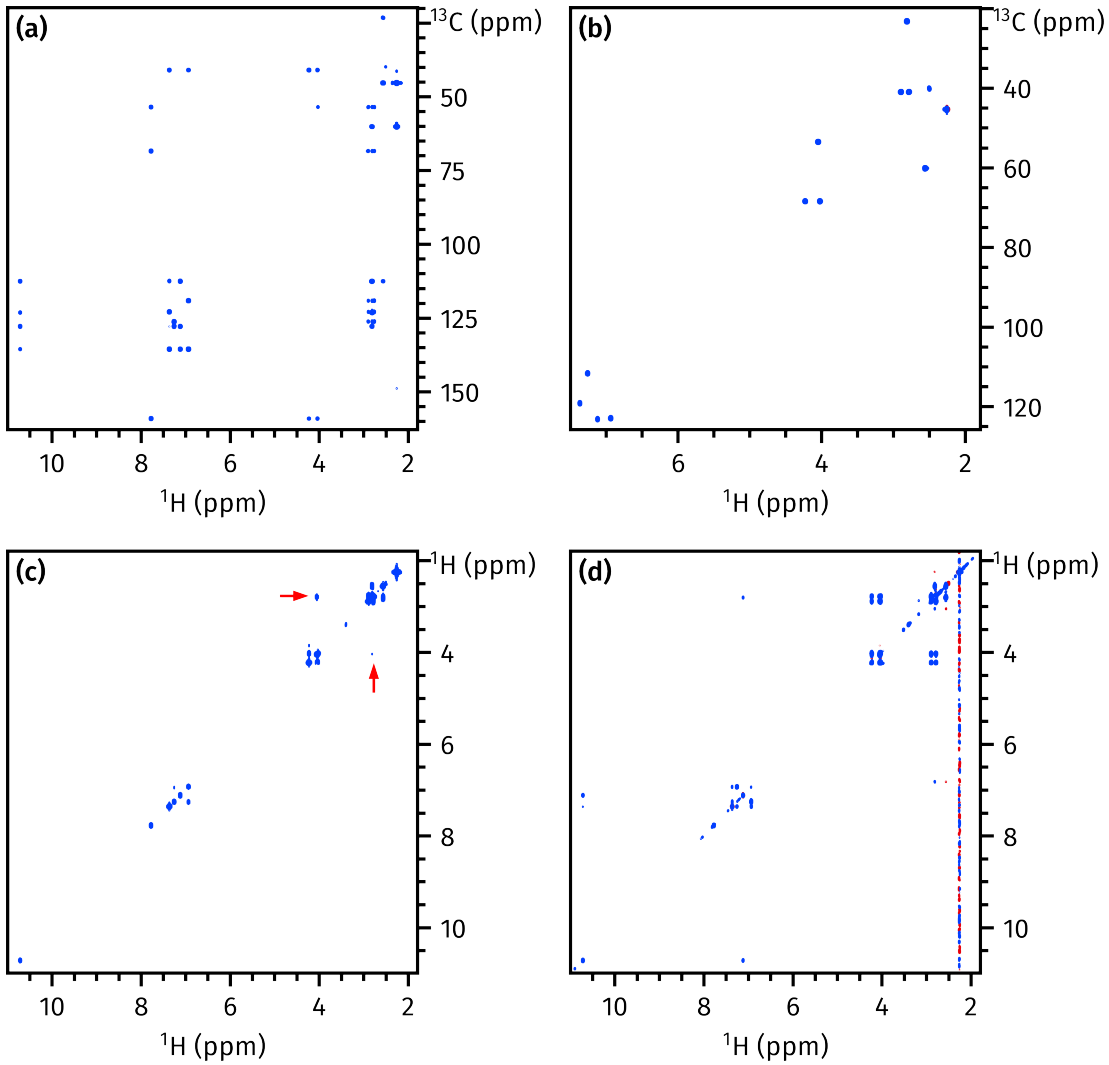

figbsbtcb

Figure 4.5: Spectra obtained from a NOAH-4 BSCT supersequence. **(a)** HMBC. **(b)** HSQC. **(c)** COSY; a pair of asymmetric crosspeaks are highlighted with red arrows. **(d)** TOCSY (60 ms DIPSI-2 mixing). Despite the COSY and TOCSY having only ~ 30% sensitivity compared to standalone experiments, the intensity of the spectra obtained is still perfectly acceptable (the contour levels chosen are 1–2 orders of magnitude larger than for the HMBC). *Data code:* `7Z-220224`.

NOAH-5 BS^{+}_{N}SCT: HMBC + ^{15}N seHSQC + HSQC + COSY + TOCSY

As the final example, we add a further magnetisation pool to the mix, namely protons directly coupled to ^{15}N (i.e. $^{1}H^{N}$). As of the time of writing, the implementation of multiple-FID experiments on Bruker spectrometers limits N to a maximum of 5, so a supersequence such as the present NOAH-5 BS^{+}_{N}SCT is the current limit. (However, there is no *scientific* argument forbidding $N > 5$, and it is likely that in future versions of TopSpin this restriction will be lifted.)

The values of A for each module are given in entry 6 of table 4.2. If the HMBC module is placed at the beginning of the supersequence, then in order to preserve *both* $^{1}H^{N}$ and $^{1}H^{C}$ magnetisation, the *zz*-filter must be extended to include ^{15}N pulses.[46] As before, the ^{15}N seHSQC and ^{13}C HSQC modules both suffer drops in sensitivity. For the ^{15}N seHSQC, this is partly because of imperfect preservation of $^{1}H^{N}$ magnetisation by the HMBC, but also stems from the addition of the *zz* isotope-selective pulse (ZIP) element to the seHSQC pulse sequence; this is described further in § 4.3.2. On the other hand, for the ^{13}C HSQC, the sensitivity loss stems purely from imperfect retention of $^{1}H^{C}$ magnetisation. Finally, because the HMBC dephases $^{1}H^{!X}$ magnetisation, the COSY and TOCSY at the end have lower sensitivities: however, as discussed above, this is not an issue in practice.

It is also possible to move the ^{15}N seHSQC module to the front: this gives it a slightly greater sensitivity, at the cost of the HMBC (entry 7, table 4.2). In general, these two modules tend to have comparable sensitivity, and which of these two arrangements is better depends on which module the sensitivity needs to be prioritised for.

Lastly, the value of ρ_t given here of 3.74 represents an effective upper limit on the time-saving factor. Although ρ_t increases with N, the extent to which it deviates from the ideal value of N also increases: it is very difficult to obtain $\rho_t > 4$, even with five modules in the supersequence. Of course, it is possible to increase ρ_t further by lengthening the recovery delay d_1 used for the experiments: for example, if d_1 is increased to 2 s from its present value of 1.5 s, ρ_t increases to 3.94. Obviously, this can only be pushed so far before it becomes meaningless.

4.2 GENESIS: automated pulse programme creation

sec:noah__genesis

I think it makes sense to start with GENESIS;[3] that way everything else can be placed in context.

It's true that this was a full paper, but it included a lot of stuff which wasn't about the website itself—these will go into later sections.

4.3 Discussion of individual modules

sec:noah__modules

4.3.1 ^{13}C sensitivity-enhanced HSQC

subsec:noah__sehsqc_c

^{13}C seHSQC

4.3.2 ^{15}N sensitivity-enhanced HSQC

subsec:noah__sehsqc_n

^{15}N seHSQC

4.3.3 HMQC

subsec:noah__hmqc

Suppression of wing artefacts (GENESIS paper)

4.3.4 HSQC-TOCSY

subsec:noah__hsqctocsy

HSQC + DIPSI + HSQC combos

Extension to HSQC-TOCSY

Cite ASAP work (Luy)

4.3.5 HSQC-COSY

subsec:noah__hsqccosy

Comparison of several versions of HSQC-COSY (JACS Au SI)

4.3.6 2DJ and PSYCHE

subsec:noah__2djpsyche

cnst37 scaling

SAPPHIRE

4.3.7 HMBC

subsec:noah__hmbc

Suppression of $^{1}J_{CH}$ artefacts (GENESIS paper)

Investigation of gradient schemes (no difference was really observed, but that's fine)

Also ^{15}N HMBC

4.3.8 ADEQUATE

subsec:noah__adequate

Recent stuff.

4.4 Solvent suppression in NOAH

sec:noah__solvsupp

GENESIS paper.

4.5 Parallel and generalised NOAH supersequences

sec:noah__parallel

Blah.

4.6 References

Yong2021JMR (1) Yong, J. R. J.; Hansen, A. L.; Kupče, Ē.; Claridge, T. D. W. Increasing sensitivity and versatility in NMR supersequences with new HSQC-based modules. *J. Magn. Reson.* **2021**, *329*, 107027, DOI: 10.1016/j.jmr.2021.107027.

Kupce2021JACSA (2) Kupče, Ē.; Yong, J. R. J.; Widmalm, G.; Claridge, T. D. W. Parallel NMR Supersequences: Ten Spectra in a Single Measurement. *JACS Au* **2021**, *1*, 1892–1897, DOI: 10.1021/jacsau.1c00423.

Yong2022AC (3) Yong, J. R. J.; Kupče, Ē.; Claridge, T. D. W. Modular Pulse Program Generation for NMR Supersequences. *Anal. Chem.* **2022**, *94*, 2271–2278, DOI: 10.1021/acs.analchem.1c04964.

Yong2022_ABBS (4) Yong, J. R. J.; Kupče, Ē.; Claridge, T. D. W. Uniting Low- and High-Sensitivity Experiments through Generalised NMR Supersequences. **2022**, manuscript in preparation.

Kupce2021NRMP (5) Kupče, Ē.; Frydman, L.; Webb, A. G.; Yong, J. R. J.; Claridge, T. D. W. Parallel nuclear magnetic resonance spectroscopy. *Nat. Rev. Methods Primers* **2021**, *1*, No. 27, DOI: 10.1038/s43586-021-00024-3.

Yong2022RSCBook (6) Yong, J. R. J.; Kupče, Ē.; Claridge, T. D. W. In *Fast 2D solution-state NMR: concepts and applications*, Giraudeau, P., Dumez, J.-N., Eds., forthcoming, 2022.

Barna1987JMR (7) Barna, J. C. J.; Laue, E. D.; Mayger, M. R.; Skilling, J.; Worrall, S. J. P. Exponential sampling, an alternative method for sampling in two-dimensional NMR experiments. *J. Magn. Reson.* **1987**, *73*, 69–77, DOI: 10.1016/0022-2364(87)90225-3.

Kazimierczuk2010PNMRS (8) Kazimierczuk, K.; Stanek, J.; Zawadzka-Kazimierczuk, A.; Koźmiński, W. Random sampling in multidimensional NMR spectroscopy. *Prog. Nucl. Magn. Reson. Spectrosc.* **2010**, *57*, 420–434, DOI: 10.1016/j.pnmrs.2010.07.002.

Mobli2014PNMRS (9) Mobli, M.; Hoch, J. C. Nonuniform sampling and non-Fourier signal processing methods in multidimensional NMR. *Prog. Nucl. Magn. Reson. Spectrosc.* **2014**, *83*, 21–41, DOI: 10.1016/j.pnmrs.2014.09.002.

Kazimierczuk2015MRC (10) Kazimierczuk, K.; Orekhov, V. Non-uniform sampling: post-Fourier era of NMR data collection and processing. *Magn. Reson. Chem.* **2015**, *53*, 921–926, DOI: 10.1002/mrc.4284.

eSunninghausen2014JACS (11) Schulze-Sünninghausen, D.; Becker, J.; Luy, B. Rapid Heteronuclear Single Quantum Correlation NMR Spectra at Natural Abundance. *J. Am. Chem. Soc.* **2014**, *136*, 1242–1245, DOI: 10.1021/ja411588d.

Schanda2006JACS (12) Schanda, P.; Van Melckebeke, H.; Brutscher, B. Speeding Up Three-Dimensional Protein NMR Experiments to a Few Minutes. *J. Am. Chem. Soc.* **2006**, *128*, 9042–9043, DOI: 10.1021/ja062025p.

Kupce2007MRC (13) Kupče, Ē.; Freeman, R. Fast multidimensional NMR by polarization sharing. *Magn. Reson. Chem.* **2007**, *45*, 2–4, DOI: 10.1002/mrc.1931.

Schanda2009PNMRS (14) Schanda, P. Fast-pulsing longitudinal relaxation optimized techniques: Enriching the toolbox of fast biomolecular NMR spectroscopy. *Prog. Nucl. Magn. Reson. Spectrosc.* **2009**, *55*, 238–265, DOI: 10.1016/j.pnmrs.2009.05.002.

Frydman2002PNASUSA (15) Frydman, L.; Scherf, T.; Lupulescu, A. The acquisition of multidimensional NMR spectra within a single scan. *Proc. Natl. Acad. Sci. U. S. A.* **2002**, *99*, 15858–15862, DOI: 10.1073/pnas.252644399.

Pelupessy2003JACS (16) Pelupessy, P. Adiabatic Single Scan Two-Dimensional NMR Spectrocopy. *J. Am. Chem. Soc.* **2003**, *125*, 12345–12350, DOI: 10.1021/ja034958g.

Frydman2003JACS (17) Frydman, L.; Lupulescu, A.; Scherf, T. Principles and Features of Single-Scan Two-Dimensional NMR Spectroscopy. *J. Am. Chem. Soc.* **2003**, *125*, 9204–9217, DOI: 10.1021/ja030055b.

Tal2010PNMRS (18) Tal, A.; Frydman, L. Single-scan multidimensional magnetic resonance. *Prog. Nucl. Magn. Reson. Spectrosc.* **2010**, *57*, 241–292, DOI: 10.1016/j.pnmrs.2010.04.001.

Gouilleux2018ARNMRS (19) Gouilleux, B.; Rouger, L.; Giraudeau, P. Ultrafast 2D NMR: Methods and Applications. *Annu. Rep. NMR Spectrosc.* **2018**, 75–144, DOI: 10.1016/bs.arnmr.2017.08.003.

Kupce2003JMR (20) Kupče, Ē.; Freeman, R. Two-dimensional Hadamard spectroscopy. *J. Magn. Reson.* **2003**, *162*, 300–310, DOI: 10.1016/s1090-7807(02)00196-9.

Kupce2003PNMRS (21) Kupče, E.; Nishida, T.; Freeman, R. Hadamard NMR spectroscopy. *Prog. Nucl. Magn. Reson. Spectrosc.* **2003**, *42*, 95–122, DOI: 10.1016/s0079-6565(03)00022-0.

Jeannerat2000MRC (22) Jeannerat, D. High resolution in the indirectly detected dimension exploiting the processing of folded spectra. *Magn. Reson. Chem.* **2000**, *38*, 415–422, DOI: 10.1002/1097-458x(200006)38:6<415::aid-mrc665>3.0.co;2-u.

Bermel2009JACS (23) Bermel, W.; Bertini, I.; Felli, I. C.; Pierattelli, R. Speeding Up ^{13}C Direct Detection Biomolecular NMR Spectroscopy. *J. Am. Chem. Soc.* **2009**, *131*, 15339–15345, DOI: 10.1021/ja9058525.

Njock2010C (24) Njock, G. B. B.; Pegnyemb, D. E.; Bartholomeusz, T. A.; Christen, P.; Vitorge, B.; Nuzillard, J.-M.; Shivapurkar, R.; Foroozandeh, M.; Jeannerat, D. Spectral Aliasing: A Super Zoom for 2D-NMR Spectra. Principles and Applications. *Chimia* **2010**, *64*, 235, DOI: 10.2533/chimia.2010.235.

Nolis2007ACIE (25) Nolis, P.; Pérez-Trujillo, M.; Parella, T. Multiple FID Acquisition of Complementary HMBC Data. *Angew. Chem. Int. Ed.* **2007**, *46*, 7495–7497, DOI: 10.1002/anie.200702258.

Parella2010CMR (26) Parella, T.; Nolis, P. Time-shared NMR experiments. *Concepts Magn. Reson.* **2010**, *36A*, 1–23, DOI: 10.1002/cmr.a.20150.

Kupce2006JACS (27) Kupče, Ē.; Freeman, R.; John, B. K. Parallel Acquisition of Two-Dimensional NMR Spectra of Several Nuclear Species. *J. Am. Chem. Soc.* **2006**, *128*, 9606–9607, DOI: 10.1021/ja0634876.

Kupce2008JACS (28) Kupče, Ē.; Freeman, R. Molecular Structure from a Single NMR Experiment. *J. Am. Chem. Soc.* **2008**, *130*, 10788–10792, DOI: 10.1021/ja8036492.

Kovacs2016MRC (29) Kovacs, H.; Kupče, Ē. Parallel NMR spectroscopy with simultaneous detection of1H and19F nuclei. *Magn. Reson. Chem.* **2016**, *54*, 544–560, DOI: 10.1002/mrc.4428.

Kupce2017ACIE (30) Kupče, Ē.; Claridge, T. D. W. NOAH: NMR Supersequences for Small Molecule Analysis and Structure Elucidation. *Angew. Chem. Int. Ed.* **2017**, *56*, 11779–11783, DOI: 10.1002/anie.201705506.

Kupce2021PNMRS (31) Kupče, Ē.; Mote, K. R.; Webb, A.; Madhu, P. K.; Claridge, T. D. W. Multiplexing experiments in NMR and multi-nuclear MRI. *Prog. Nucl. Magn. Reson. Spectrosc.* **2021**, *124–125*, 1–56, DOI: 10.1016/j.pnmrs.2021.03.001.

Nagy2019CC (32) Nagy, T. M.; Gyöngyösi, T.; Kövér, K. E.; Sørensen, O. W. BANGO SEA XLOC/HMBC–H2OBC: complete heteronuclear correlation within minutes from one NMR pulse sequence. *Chem. Commun.* **2019**, *55*, 12208–12211, DOI: 10.1039/c9cc06253j.

Nagy2020JMR (33) Nagy, T. M.; Kövér, K. E.; Sørensen, O. W. Double and adiabatic BANGO for concatenating two NMR experiments relying on the same pool of magnetization. *J. Magn. Reson.* **2020**, *316*, 106767, DOI: 10.1016/j.jmr.2020.106767.

Nagy2021ACIE (34) Nagy, T. M.; Kövér, K. E.; Sørensen, O. W. NORD: NO Relaxation Delay NMR Spectroscopy. *Angew. Chem. Int. Ed.* **2021**, *60*, 13587–13590, DOI: 10.1002/anie.202102487.

Timari2022CC (35) Timári, I.; Nagy, T. M.; Kövér, K. E.; Sørensen, O. W. Synergy and sensitivity-balance in concatenating experiments in NO relaxation delay NMR (NORD). *Chem. Commun.* **2022**, *58*, 2516–2519, DOI: 10.1039/d1cc06663c.

Orts2018M (36) Orts, J.; Gossert, A. D. Structure determination of protein-ligand complexes by NMR in solution. *Methods* **2018**, *138-139*, 3–25, DOI: 10.1016/j.ymeth.2018.01.019.

zeSunninghausen2017JMR (37) Schulze-Sünninghausen, D.; Becker, J.; Koos, M. R. M.; Luy, B. Improvements, extensions, and practical aspects of rapid ASAP-HSQC and ALSOFAST-HSQC pulse sequences for

studying small molecules at natural abundance. *J. Magn. Reson.* **2017**, *281*, 151–161, DOI: 10.1016/j.jmr.2017.05.012.

Vitorge2010JMR (38) Vitorge, B.; Bodenhausen, G.; Pelupessy, P. Speeding up nuclear magnetic resonance spectroscopy by the use of SMAll Recovery Times – SMART NMR. *J. Magn. Reson.* **2010**, *207*, 149–152, DOI: 10.1016/j.jmr.2010.07.017.

Shaw1996JMRSA (39) Shaw, A. A.; Salaun, C.; Dauphin, J.-F.; Ancian, B. Artifact-Free PFG-Enhanced Double-Quantum-Filtered COSY Experiments. *J. Magn. Reson., Ser. A* **1996**, *120*, 110–115, DOI: 10.1006/jmra.1996.0105.

Howe2014MRC (40) Howe, P. W. A. Rapid pulsing artefacts in pulsed-field gradient double-quantum filtered COSY spectra. *Magn. Reson. Chem.* **2014**, *52*, 329–332, DOI: 10.1002/mrc.4060.

Claridge2019MRC (41) Claridge, T. D. W.; Mayzel, M.; Kupče, Ē. Triplet NOAH supersequences optimised for small molecule structure characterisation. *Magn. Reson. Chem.* **2019**, *57*, 946–952, DOI: 10.1002/mrc.4887.

Haasnoot1984JMR (42) Haasnoot, C. A. G.; van de Ven, F. J. M.; Hilbers, C. W. COCONOSY. Combination of 2D correlated and 2D nuclear overhauser enhancement spectroscopy in a single experiment. *J. Magn. Reson.* **1984**, *56*, 343–349, DOI: 10.1016/0022-2364(84)90114-8.

Gurevich1984JMR (43) Gurevich, A. Z.; Barsukov, I. L.; Arseniev, A. S.; Bystrov, V. F. Combined COSY-NOESY experiment. *J. Magn. Reson.* **1984**, *56*, 471–478, DOI: 10.1016/0022-2364(84)90311-1.

Nolis2019MRC (44) Nolis, P.; Parella, T. Practical aspects of the simultaneous collection of COSY and TOCSY spectra. *Magn. Reson. Chem.* **2019**, *57*, S85–S94, DOI: 10.1002/mrc.4835.

Kupce2018CC (45) Kupče, Ē.; Claridge, T. D. W. Molecular structure from a single NMR supersequence. *Chem. Commun.* **2018**, *54*, 7139–7142, DOI: 10.1039/c8cc03296c.

Kupce2019JMR (46) Kupče, Ē.; Claridge, T. D. W. New NOAH modules for structure elucidation at natural isotopic abundance. *J. Magn. Reson.* **2019**, *307*, 106568, DOI: 10.1016/j.jmr.2019.106568.

refsection:5